Cellular and Molecular Life Sciences (2019) 76:1807–1819
https://doi.org/10.1007/s00018-019-03027-2

ORIGINAL ARTICLE

Expression and purification of recombinant extracellular sulfatase HSulf-2 allows deciphering of enzyme sub-domain coordinated role for the binding and 6-*O*-desulfation of heparan sulfate

Amal Seffouh[1] · Rana El Masri[1] · Olga Makshakova[2] · Evelyne Gout[1] · Zahra el Oula Hassoun[1] · Jean-pierre Andrieu[1] · Hugues Lortat-Jacob[1] · Romain R. Vivès[1,3]

Received: 4 December 2018 / Revised: 8 January 2019 / Accepted: 25 January 2019 / Published online: 20 February 2019
© Springer Nature Switzerland AG 2019

Abstract

Through their ability to edit 6-*O*-sulfation pattern of Heparan sulfate (HS) polysaccharides, Sulf extracellular endosulfatases have emerged as critical regulators of many biological processes, including tumor progression. However, study of Sulfs remains extremely intricate and progress in characterizing their functional and structural features has been hampered by limited access to recombinant enzyme. In this study, we unlock this critical bottleneck, by reporting an efficient expression and purification system of recombinant HSulf-2 in mammalian HEK293 cells. This novel source of enzyme enabled us to investigate the way the enzyme domain organization dictates its functional properties. By generating mutants, we confirmed previous studies that HSulf-2 catalytic (CAT) domain was sufficient to elicit arylsulfatase activity and that its hydrophilic (HD) domain was necessary for the enzyme 6-*O*-endosulfatase activity. However, we demonstrated for the first time that high-affinity binding of HS substrates occurred through the coordinated action of both domains, and we identified and characterized 2 novel HS binding sites within the CAT domain. Altogether, our findings contribute to better understand the molecular mechanism governing HSulf-2 substrate recognition and processing. Furthermore, access to purified recombinant protein opens new perspectives for the resolution of HSulf structure and molecular features, as well as for the development of Sulf-specific inhibitors.

Keywords Glycosaminoglycan · Structure–function relationships · Extracellular matrix · Glycocalyx · Heparin

Introduction

Sulfs are sulfatases that catalyze the regioselective hydrolysis of 6-*O*-sulfate groups on heparan sulfate (HS) polysaccharides. Since their discovery in 2001 [1], accumulating evidence has highlighted Sulfs as unique members amongst sulfatases, differentiating by their extracellular localization, distinct structural organization, enzymatic activity at neutral pH, and biological role as major modulator of HS function rather than mere actor of the polysaccharide recycling metabolism. HS is a linear sulfated polysaccharide of the Glycosaminoglycan (GAG) family, which is abundantly found at the cell surface and in the extracellular matrix (ECM) of most animal tissues. It is involved in many biological processes, through its ability to bind and modulate a vast repertoire of proteins, including growth factors, cytokines and morphogens, etc. [2–4]. These large interactive properties are essentially governed by specialized saccharide regions of the polysaccharide termed S-domains.

Amal Seffouh and Rana El Masri contributed equally to this work.

Electronic supplementary material The online version of this article (https://doi.org/10.1007/s00018-019-03027-2) contains supplementary material, which is available to authorized users.

✉ Romain R. Vivès
romain.vives@ibs.fr

[1] Univ. Grenoble Alpes, CNRS, CEA, IBS, 38000 Grenoble, France

[2] Kazan Institute of Biochemistry and Biophysics, FRC Kazan Scientific Center of RAS, Kazan, Russian Federation

[3] IBS, 71 Avenue des Martyrs CS 10090, 38044 Grenoble Cedex 9, France

In S-domains, the original repeated *N*-acetyl glucosamine (GlcNAc)–Glucuronic acid (GlcA) disaccharide motif is extensively modified. Glucosamines are *N*-sulfated (GlcNS), GlcA can be epimerized into iduronic acid (IdoA), and *O*-sulfation can occur at C2 of IdoA, as well as at C6 (and more rarely C3) of glucosamines. Addition and distribution of sulfate groups as well as uronic acid (UA) epimers is catalyzed by stepwise series of highly regulated enzyme reaction during HS biosynthesis (for review see [5, 6]). Sulfs contribute to further regulate the polysaccharide structure, by editing HS 6-*O*-sulfation status. These enzymes show strong specificity for highly sulfated disaccharide units, which are mostly present within the inner regions of the HS functional S-domains. Hence, although Sulf-driven desulfation is structurally subtle, it dramatically affects HS function by modulating its ability to interact with many protein ligands. Consequently, Sulfs have been associated with a number of physiopathological processes, including embryo development, tissue regeneration, cancer and neurodegenerative disease [7–9].

Sulf isoforms (Sulf-1 and Sulf-2) and orthologs share a very similar molecular organization, including 2 regions that are essential for enzyme activity: the catalytic domain (CAT) and the basic/hydrophilic domain (HD) [10–12]. Sulf CAT domain displays strong homology with other mammalian sulfatases and comprises notably strictly conserved residues involved in arylsulfatase active site, including a posttranslationally modified cysteine into an *N*-formylglycine (FGly) residue. In contrast, the HD domain is a unique feature of these enzymes and is involved in high-affinity interaction with HS substrates. This domain shows no sequence homology with any other known protein, limited secondary structure prediction and poor sequence conservation amongst Sulfs, thereby suggesting that it may confer isoform-dependent substrate-binding specificities to the enzyme. Within HS, Sulfs primarily target [UA(2S)-GlcNS(6S)] trisulfated disaccharides, although limited activity has also been reported on [UA-GlcNS(6S)] disulfated disaccharide species [11, 13, 14]. However, a wealth of evidence reported divergent activities of Sulf isoforms, notably in cancer, and studies on mouse Sulf-1 and Sulf-2 KO mice have highlighted differences in HS sulfation patterns [15–17]. Altogether, these suggest that substrate specificities of the Sulfs may not be restricted to monosaccharide or disaccharide units, but may most likely involve the recognition of much longer saccharide motifs. Recently, we have shown that human Sulfs (HSulfs) catalyzed the 6-*O*-desulfation of HS through an original, orientated and processive mechanism [13]. We speculated that this unique mechanism involved the coordinated actions of both CAT and HD domains: the HD domain would provide substrate binding and specificity, direct proper presentation to the CAT domain and drive processivity through multiple and transient interaction with HS that would allow the enzyme to "glide" along the polysaccharide chain. In agreement with this, other studies have since shown that HSulf-1 substrate recognition was complex and involved multiple interaction events with different binding sites present within the HD domain, which provided unique dynamic properties [18]. More recently, a study on HSulf-1 showed that HD/HS binding was found to exhibit atypical catch-bond type properties, with increased lifetime when subjected to external forces [19].

However, and despite growing interest, Sulfs are highly elusive enzymes, and getting structural and molecular insights into the enzymatic mechanism remains a major scientific challenge. Such studies have primarily been hampered by limited availability of recombinant enzyme. Sulfs cannot be expressed in bacteria, as the enzyme requires post-translational modifications for activity, notably *N*-glycosylations, furin cleavage maturation and formation of the catalytic FGly residue. Recovery of Sulfs from naturally expressing or transfected mammalian cells has been achieved by us and others, but only as concentrated conditioned medium preparations, as low protein yields precluded any purification attempts. In the present study, we report for the first time the preparation of purified, recombinant HSulf-2 in mammalian cells. Access to this source of enzyme enabled us to investigate further the respective roles of Sulf domains in the enzyme catalytic activities and substrate recognition process. Using heparin-bead crosslinking experiments, we identified 2 novel HS binding epitopes within the enzyme CAT domain, and we analyzed the contribution of these epitopes in the enzyme functional properties, including: (i) its arylsulfatase activity (imparted by the sulfatase-conserved active site); (ii) endosulfatase activity (Sulf-specific ability to 6-*O*-desulfate HS and heparin); (iii) and its ability to bind to heparin and HS with high affinity. Based on the data obtained, we propose here a refined model of HS 6-*O*-desulfation process by the Sulfs, which may help understanding further this complex regulatory mechanism of HS function.

Materials and methods

Unless specified otherwise, all chemicals and reagents were from Sigma.

Production of recombinant WT and mutant HSulf-2

HSulf-2 coding sequence (Genbank CR749319.1, cDNA in pcDNA3.1 plasmid was courtesy of Professor S. Rosen, University of California, USA) was amplified by PCR (for primer sequences, see Supplementary experimental 1), then inserted through EcoRV/XmaI restriction sites in a pcDNA3.1/Myc-His(-) vector modified to express proteins

of interest between TEV cleavable SNAP and 6His tags at the N- and C-terminus, respectively (gift from P. Desprès, Institut Pasteur, France). Mutants were generated from this vector by the Robiomol platform of Integrated Structural Biology Grenoble (ISBG).

WT and mutant encoding vectors were used to stably transfect FreeStyle HEK 293-F cells (medium and tissue culture reagents from Thermo fisher scientific), as previously described [13]. Protein productions were achieved by seeding cells at a 10^6/mL density in FreeStyle 293 Expression Medium, then harvesting conditioned medium (CM) 5 days later. Full-length protein purification was achieved in two steps of cation-exchange and size-exclusion chromatographies. Conditioned medium (CM) was first loaded onto a SP-Sepharose column (GE healthcare) equilibrated in 50 mM Tris, 5 mM $CaCl_2$, 5 mM $MgCl_2$, 100 mM NaCl, pH 7.5, at a flow rate of 0.5 mL/min. After washing the column with the same buffer, proteins were eluted with a NaCl gradient (from 100 mM to 1 M). Fractions corresponding to the absorbance peak at 280 nm (0.5 mL/fraction) were collected, pooled and concentrated on a 30-kDa centrifugal unit (Centricon-30, Millipore). Concentrated samples (200 µl) were then injected onto a Superdex-200 column (GE healthcare) equilibrated with 50 mM Tris, 5 mM $CaCl_2$, 5 mM $MgCl_2$, 300 mM NaCl, pH 7.5, at a flow rate of 0.5 mL/min. As previously, 0.5 mL fractions were collected, pooled and concentrated.

Purification of HSulf-2ΔHD (and mutants) was performed by affinity chromatography, using a nickel column (Thermo fisher scientific). CM was loaded onto a nickel resin equilibrated in 50 mM Tris buffer, 5 mM $CaCl_2$, 5 mM $MgCl_2$, 100 mM NaCl, pH 7.5. Protein was eluted from the column with 50 mM Tris buffer, 5 mM $CaCl_2$, 5 mM $MgCl_2$, 100 mM NaCl 350 mM imidazole, pH 7.5, then concentrated on Centricon-30, with repeated washings of the centrifugal unit with equilibration buffer to achieve complete removal of imidazole.

Purified proteins were supplemented with anti-proteases (Complete EDTA-Free, Roche), 20% glycerol, quantified and stored at − 20 °C. Detection after PAGE analysis was performed in reducing conditions, using standard protocols of Coomassie blue staining, Western-blotting with a primary goat polyclonal anti N-terminal HSulf-2 antibody (A-18, Santa-Cruz biotechnology, dil. 1/1000), or detection of the SNAP tag using SNAP fluorescent ligand SNAP-Vista Green (New England Biolabs).

Heparin-bead cross-linking experiments

Heparin-bead cross-linking analysis was performed as described previously [20]. Briefly, heparin-beads were activated with a mixture of 40 mM l-ethyl-3-(3-dimethylaminopropyl) carbodiimide (EDC), 10 mM *N*-hydroxysuccinimide (NHS) in 50 mM MES and 150 mM NaCl pH5.5, for 10 min at room temperature (RT). EDC/NHS in excess were inactivated by addition of ß-mercaptoethanol (15 mM final) and removed by three steps of centrifugation/washing of the beads with PBS. Heparin-beads were then incubated with 35 µg (~ 1 µM) of recombinant HSulf-2 in PBS for 2 h at RT, under gentle agitation. After quenching the reaction by addition of primary amine containing buffer (100 mM Tris, final concentration), beads were rinsed with PBS, 2 M NaCl to remove non-covalently bound material. Cross-linked HSulf-2 was denatured by heating the beads at 60 °C in PBS, 2 M Urea for 45 min and proteolyzed by incubation with thermolysine (53 mIU) at 50 °C for 16 h. Released peptides were removed by three washing steps with PBS, 2 M NaCl, 15 mM ß-mercaptoethanol, 1% Triton, while heparin-bound peptides were identified by Edman degradation automated sequencing. Cross-linked amino-acids are typically identified by the presence of a "blank" cycle during the sequencing and a drop of the recovery yields for the sequencing of downstream residues.

Aryl-sulfatase assay

Arylsulfatase activity of recombinant WT and mutant HSulf-2 was assessed using the fluorogenic pseudo-substrate 4-methyl umbelliferyl sulfate (4-MUS), as described previously {Frese, 2009 #948}. Briefly, 1–3 µg of protein was incubated with 10 mM 4-MUS in 50 mM Tris 10 mM $MgCl_2$, pH 7.5 for 1–4 h at 37 °C. Reaction was monitored by fluorescence measurement (excitation 360 nm, emission 465 nm).

Endosulfatase assay

Heparin (25 µg) was incubated with 3 µg of recombinant WT or mutant HSulf-2 in 50 µl of 50 mM Tris and 2.5 mM $MgCl_2$, pH 7.5 for 4 h. The enzyme was inactivated by heating the sample at 100 °C for 5 min, then an aliquot of the digestion products (~ 1/10) was exhaustively degraded into disaccharides by incubation with a cocktail of heparinase I, II and III (Grampian enzymes, 10 mU each) in 100 mM sodium acetate, 0.5 mM $CaCl_2$, pH 7.1 and for 48 h at 37 °C. Compositional analysis was performed by RPIP-HPLC as previously described [21]. Samples were injected onto a Phenomenex Luna 5 µm C18 reversed phase column (4.6 × 300 mm, Phenomenex) equilibrated at 0.5 mL/min in 1.2 mM tetra-*N*-butylammonium hydrogen sulfate (TBA) and 8.5% acetonitrile, then resolved using a multi-step NaCl gradient (0–30 mM in 1 min, 30–90 mM in 39 min, 90–228 mM in 2 min, 228 mM for 4 min, 228–300 mM in 2 min and 300 mM for 4 min) calibrated with HS disaccharide standards (Iduron). Post-column disaccharide derivatization was achieved by on-line addition of 2-cyanoacetamide

(0.25%) in NaOH (0.5%) at a flow rate of 0.16 mL/min, followed by fluorescence detection (excitation 346 nm, emission 410 nm).

Analysis of HSulf-2–heparin interaction by immunoassay

Binding to heparin was evaluated by an immunoassay test. Microtiter plates (black maxisorp 96wells, Nunc) were coated overnight at 4 °C with 1 mg/mL of streptavidin in 50 mM Tris–Cl and 150 mM NaCl, pH 7.5 (TBS) buffer. Plates were washed with TBS and then incubated with biotinylated heparin (1 mg/mL) prepared as described (Supplementary experimental 2), in TBS for 1 h at RT (100 µl/well). After blocking for 1 h at RT with TBS, 2% BSA, recombinant HSulf-2 variants were added to the wells at different concentrations in TBS 0.05% (w/v) tween 20 (TBS-T) and incubated at 4 °C for 2 h. Wells were washed with TBS-T and then incubated with rabbit polyclonal anti-HSulf-2 (gift from K. Uchimura, 1/1000 dilution) in TBS-T (for full-length HSulf-2), or with anti penta-HIS antibody for HSulf-2ΔHD variants (Qiagen, 1/100 dilution), at 4 °C, for 2 h or overnight, respectively. After extensive washing, fluorescent (A488) or HRP-conjugated secondary antibodies (Jackson ImmunoResearch Laboratories, 1:1000 dilution) was added for 1 h at 4 °C. Wells were washed again prior to fluorescence reading (excitation 485 nm, emission 535 nm) or treated with ECL (Thermo fisher scientific) for luminescence measurement.

Analysis of HSulf-2–heparin interaction by SPR

All experiments were performed on a BIAcore T200 (GE healthcare). Biotinylated heparin (See Supplementary experimental 2) was immobilized on a S-CM4 sensorchip, as described before [22]. Briefly, two sensorchip flow-cells were activated with a mix of 0.2 M *N*-ethyl-*N*′-(diethylaminopropyl)-carbodiimide (EDC) and 0.05 M *N*-hydroxy-succimide (NHS). Streptavidin (50 µg/mL in 10 mM acetate buffer, pH 4.5) was then injected over the activated flow cells (~ 2500 RU (Response Unit) of immobilized streptavidin). One of these flowcells served as negative control, while biotinylated heparin was injected on the other (40–50 RU of immobilized heparin). All SPR experiments were then performed, using HBS-P buffer (10 mM HEPES, 150 mM NaCl, 0.05% surfactant P20, pH 7.4) supplemented with 0.02 M EDTA), at a flow rate of 10–50 µl/min. Interaction assays involved 5-min injections of 0–40 nM HSulf-2 (WT and mutant) over the heparin and negative control surfaces, followed by a 5-min washing step with HBS-P buffer to allow dissociation of the complexes formed. At the end of each cycle, the heparin surface was regenerated by a 2.5-min injection of 2 M NaCl. Sensorgrams shown correspond to on-line subtraction of the negative control to the heparin surface signal.

Molecular modeling

For homology modeling, the sequence of HSulf-2ΔHD truncated form shown in Supplementary (Supp. Figure 2) was taken. Multiple alignment with arylsulfatase of known crystal structure (A, B and C, pdb id: 1auk, 1p49 and 1fsu, correspondingly) was performed using ClustalW algorithm to determine conservative fragments in the HSulf sequence. The HSulf-2ΔHD model was built using Modeller [23] and arylsulfatase A was chosen as a template due to its best resolution (2.1 Å). The conservative core folding was kept as in the template structure whilst the structurally variable regions including missing loops were refined. Then, the structure was repeatedly energy minimized and equilibrated in the course of short MD runs. Resulted structure was quality checked using PROCHECK online service [24].

To determine the orientation of HS towards HSulf-2ΔHD binding site, molecular docking procedure was carried out. The heparin oligosaccharide fragments GlcNS(6S)-[IdoA(2S)-GlcNS(6S)]$_n$ were used as a ligand (n amonted from 1 to 5), initial coordinates of which were taken from NMR structure of highly sulfated heparin (pdb id 1hpn). Molecular docking the HS fragments to HSulf-2ΔHD was performed using the High Ambiguity Driven biomolecular DOCKing (HADDOCK) approach [25, 26]. The algorithm allows one to perform knowledge-based docking; thus the residues determined using cross-linking mapping approach were indicated as directly involved into interaction with the ligand. The docking protocol was the following: 1000 structures were generated for initial rigid docking, then 200 of the most energetically favorable structures were subjected to semi-flexible annealing, where the parts involved in interactions were allowed to move. Afterwards, the structure of protein–ligand complexes was refined in explicit water solvent bath in the course of short molecular dynamics simulation. The most energetically favorable docking pose was taken for further analysis.

Results

Expression and purification of recombinant HSulf-2 and HSulf-2ΔHD

Purification of recombinant HSulf-2 was achieved by taking advantage of our previously reported expression system in mammalian HEK 293-F cells [13], which showed efficient protein production from high-density suspension cultures, and recovery of the secreted enzyme in low-protein, serum-free conditioned medium. For this, HSulf-2 cDNA was

inserted in a pcDNA3.1 vector modified for adding SNAP and 6His tags (at the N-ter and C-ter of HSulf-2, respectively, Fig. 1a) to facilitate protein purification and detection. We first attempted to purify the enzyme from conditioned medium by his tag affinity chromatography. However, results showed that the protein was not retained on the nickel column, even in the absence of imidazole (data not shown). We thus developed a two-step purification procedure involving cation-exchange and size-exclusion chromatographies and monitored protein elution by PAGE analysis of the collected fractions. HSulf-2 eluted from the SP-Sepharose column at ~0.4 to 0.6 M NaCL, along with other protein contaminants (Supp. Figure 1A).

Size-exclusion separation enabled recovery of pure protein (Fig. 1b, c). As reported elsewhere (Seffouh et al., submitted), only the ~95-kDa SNAP tagged N-terminal chain of the protein could be visualized by Coomassie blue staining (Fig. 1c), as confirmed by Western blotting using an anti N-terminal HSulf-2 or using a fluorescent ligand binding to the SNAP tag (Fig. 1c). However, the presence of both chains in stoichiometric abundance as well as the furin cleavage site at $R_{538}S$ was confirmed by Edman N-terminal sequencing (Supp. Figure 2). Unexpectedly, HSulf-2 eluted with a high apparent molecular weight (aMW> 1000 kDa, based on elution time), but protein aggregation and/or oligomerization was ruled out by quality control analysis of the preparation using negative staining electron microscopy (data not shown). From our data, we estimated net production yields of recombinant HSulf-2 at ~2 to 3 mg/L of culture medium and purity at 90–95%. HSulf-2 signal was also occasionally found in a second, minor, late eluting peak ($_{deg}$HSulf-2, Fig. 1b), which corresponded to degraded forms of the enzyme. As the 95-kDa band could still be visualized on PAGE analysis of the corresponding fractions, this could suggest higher sensitivity of HSulf-2 HD domain to proteolytic degradation. However, work at 4 °C and addition of antiproteases throughout the purification procedure considerably reduced the size of this second peak.

Expression of HSulf-2ΔHD in HEK293F cells was achieved similarly, but surprisingly, the protein bound

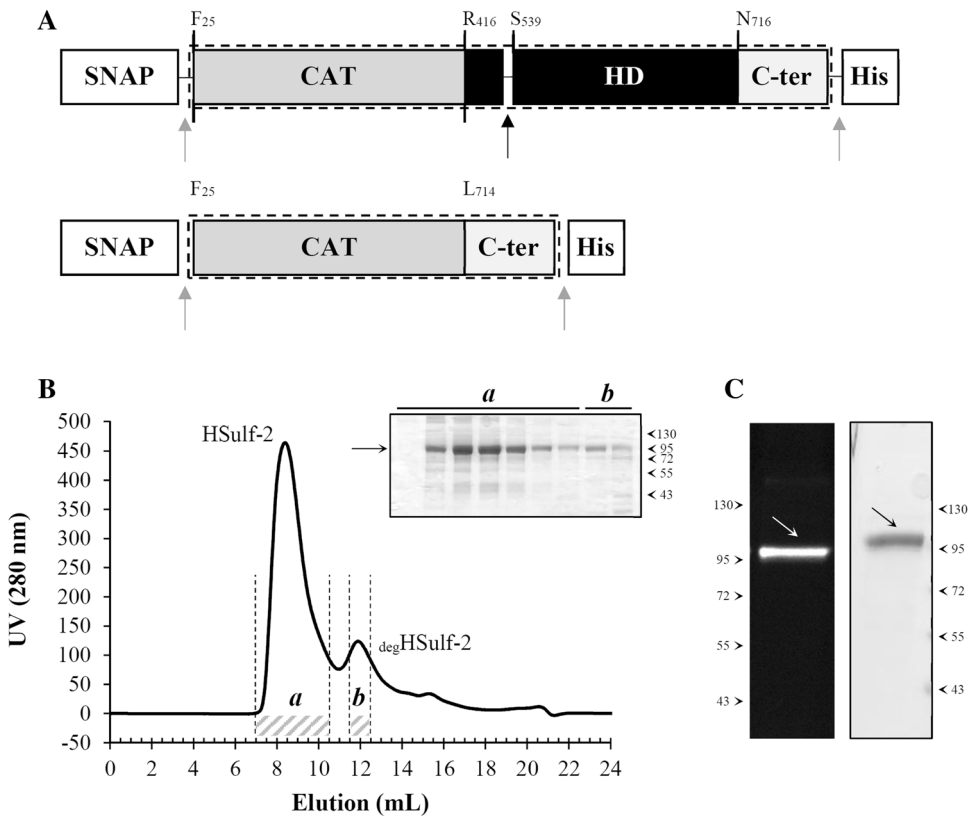

Fig. 1 Expression and purification of recombinant HSulf-2. **a** Representation of HSulf-2 and HSulf-2ΔHD constructs. Boxes represent HSulf-2 C-ter, CAT and HD domains (from light grey to black, respectively) and added SNAP and His tags (white boxes). Arrows indicate furin (black) and added-TEV (grey) cleavage sites. Amino acids (numbered according to HSulf-2 full amino acid sequence) delineating HSulf-2 domains are shown. **b** Size-exclusion separation profile of HSulf-2. Fractions corresponding to HSulf-2 (***a***) and $_{deg}$H-Sulf-2 (***b***) are indicated by grey/white dashed area and PAGE stained by Coomassie blue of these fractions are shown in the inset. The arrows indicate the band corresponding to HSulf-2 N-terminal chain. **c** Gel electrophoresis of HSulf-2 revealed by fluorescent SNAP substrate (left) and Coomassie blue (right). Arrows indicate the band corresponding to the 95 kDa SNAP-tagged N-terminal chain

efficiently to the nickel column (Supp. Figure 1B and 1C). PAGE analysis showed a single ~ 110-kDa band corresponding to the SNAP-tagged HSulf-2ΔHD (note that HSulf-2ΔHD is composed of a single polypeptide chain, as the furin cleavage site present in the HD domain is absent). An estimated ~ 90% purity was achieved using a single step His-tag affinity chromatography and production yield was significantly higher that for the Full-length enzyme (~ 8 to 10 mg/L).

Arylsulfatase, heparin binding and 6-*O*-endosulfatase activities of HSulf-2 and HSulf-2ΔHD

To validate our expression system, we next assessed the functional properties of purified recombinant HSulf-2, using three distinct biochemical assays. We first analyzed the arylsulfatase activity of recombinant HSulf-2 using the 4MUS assay, which measures the ability of arylsulfatases to convert the non-fluorescent 4-MUS pseudo-substrate into the fluorescent 4-MU product [10]. Results confirmed the ability of both enzymes to process the 4MUS, with comparable levels of fluorescence monitored after 1 h of incubation (Fig. 2a), thereby indicating that deletion of the HD domain did not compromise the integrity of the enzyme active site. Noteworthy, although both HSulf-2 and HSulf-2ΔHD catalyzed 4-MUS desulfation at very similar initial velocities, processing rate was sustained for up to 4 h for HSulf-2, but decreased after 2 h for HSulf-2ΔHD (Supp. Figure 3A).

HS binding properties of HSulf-2 and HSulf-2ΔHD were next investigated by SPR, as previously described [22]. In this assay, reducing-end biotinylated heparin (see supplementary experimental 2) is immobilized on streptavidin-coated sensorchips, a design that mimics to a certain extent the display of proteoglycan-bound HS chains at the cell surface. HSulf-2 was injected onto these functionalized surfaces, in an EDTA-supplemented buffer to prevent enzymatic degradation of the immobilized GAGs, and SPR sensorgrams of the interaction were recorded in real time. Results obtained for full length showed a very productive binding to heparin, with a slow dissociation phase suggesting formation of stable enzyme/substrate complexes (Fig. 3a). Unexpectedly, HS binding properties of HSulf-2ΔHD were not totally abolished, as lower but significant interaction to the heparin surface could still be monitored by SPR (Fig. 3a). To determine K_D and kinetic parameters for the interaction, we injected a series of HSulf-2 concentrations over the heparin surface (Fig. 3b). However, examination of the binding curves clearly indicated a complex mode of interaction and the data could not be fitted to a 1:1 Langmuir binding model. We thus analyzed the interaction using ELISA assays. Results yielded typical binding curves (Figs. 3c, d) and K_Ds were determined by Scatchard analysis. Affinities of 4.2 ± 1.2 nM and 20.4 ± 2.1 nM were calculated for full-length HSulf-2 and HSulf-2ΔHD, respectively. These results confirm the major role of the HD domain in the binding to HS, but indicate that the CAT domain on its own can bind, although with significantly lower efficiency, to HS and heparin.

We finally assessed HS 6-*O*-endosulfatase properties of the enzymes. For this, we analyzed heparin disaccharide composition, following treatment by either HSulf-2 or HSulf-2ΔHD. Data (Fig. 2b) showed that digestion with the full-length enzyme dramatically reduced heparin [ΔHexA(2S)-GlcNS(6S)] trisulfated disaccharide content (− 19% compared to untreated heparin) and concomitantly increased the level of the resulting [ΔHexA(2S)-GlcNS] disulfated disaccharide (+ 14% compared to untreated heparin). Additionally, a small but significant decrease in [ΔHexA-GlcNS(6S)] disaccharide could be observed in HSulf-2 treated heparin (− 1.4%). In contrast, HSulf-2ΔHD showed impaired 6-*O*-endosulfatase activity, with no significant changes in [ΔHexA(2S)-GlcNS(6S)] and [ΔHexA(2S)-GlcNS] composition when compared to untreated heparin.

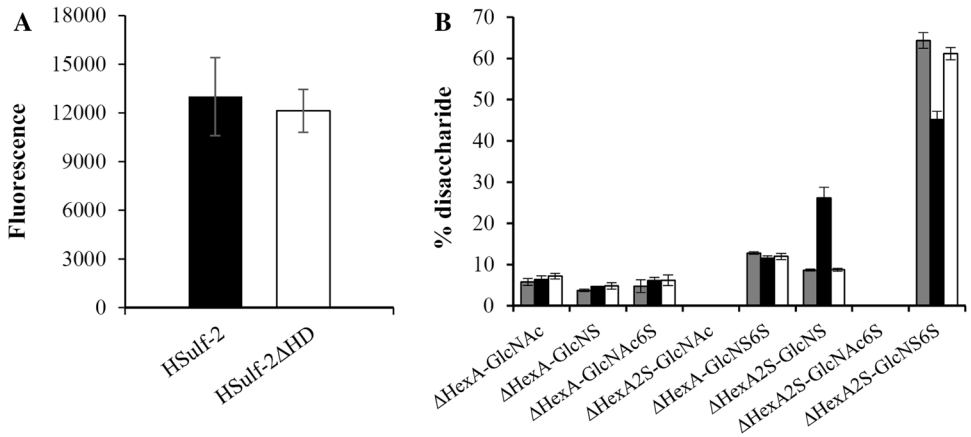

Fig. 2 Comparison of HSulf-2 and HSulf-2ΔHD arylsulfatase and endosulfatase activities. **a** Processing of 4-MUS after a 1 h digestion with HSulf-2 (black) and HSulf-2ΔHD (white). **b** Disaccharide analysis of heparin, without (grey) or after a 4 h digestion with HSulf-2 (black) or HSulf-2ΔHD (white). Error bars represent SEM of triplicate analysis

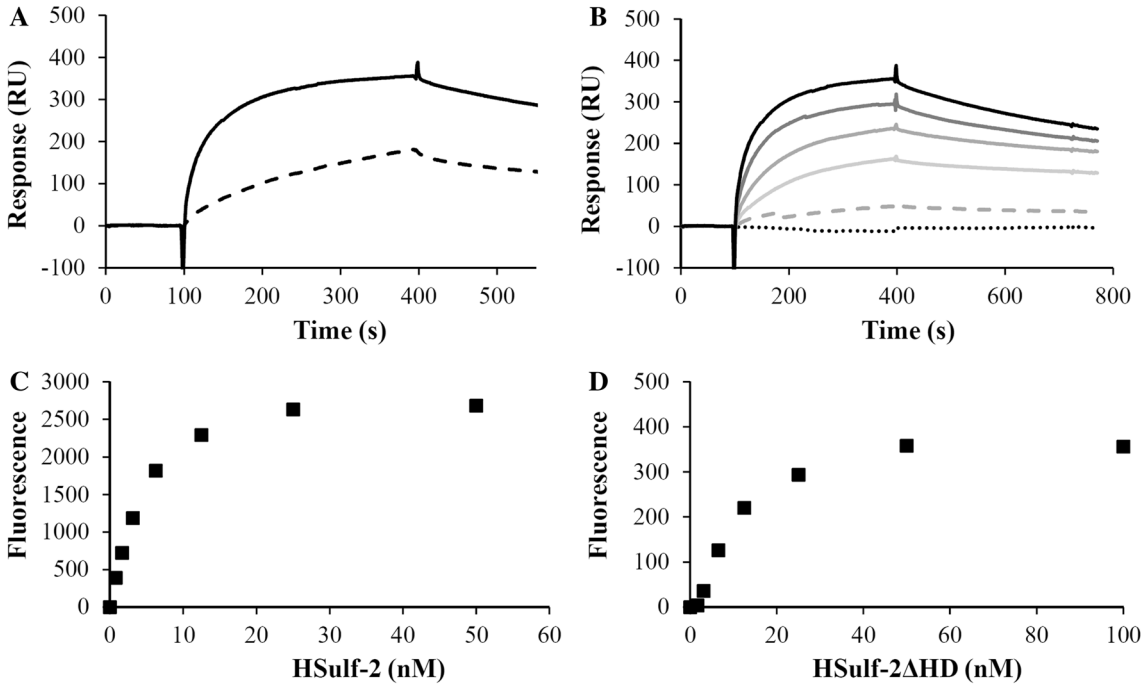

Fig. 3 Interaction of HSulf-2 and HSulf-2ΔHD with heparin. **a** SPR analysis of the binding of HSulf-2 (plain) and HSulf-2ΔHD (dashed) on a heparin-functionalized surface. **b** Injection of buffer (dashed, black line) or increasing (from dashed pale, to plain dark) 1.25–40 nM concentrations of HSulf-2 on the heparin surface. **c** Immunoassay of HSulf-2 interaction with heparin. **d** Immunoassay of HSulf-2ΔHD interaction with heparin; curves shown are representative of at least three independent experiments

Altogether, these results corroborate previously reported HSulf-2 activities, thereby confirming the functional integrity of our purified, recombinant enzyme.

Mapping of HSulf-2 HS binding sites

The development of an efficient recombinant HSulf-2 production system is an important step forward that opens wide perspectives for studying the structural and functional features of this enzyme. Here, we chose to focus on the characterization of the enzyme/substrate recognition process. We thus used an in-house developed technique to cartography heparin binding sites within proteins [20], with the aim to identify HSulf-2 amino acids involved in HS binding. This method is based on the formation of covalent complexes between the protein of interest and heparin functionalized beads, the proteolytic digestion of these complexes and the identification of the peptides remaining trapped on the polysaccharide (i.e. participating to the binding) by performing N-terminal sequencing analysis directly on the beads.

Analysis of HSulf-2 using this approach yielded data with unusually high background (i.e. amino acids that could not be confidently attributed to any sequence within HSulf-2) and a rapid drop of recovery yields at each sequencing cycle. Peptides located within the HD domain could be detected, but these results were erratic and poorly reliable. In contrast, the approach consistently highlighted two short peptides within the enzyme CAT domain: V_{179}KEK and L_{401}KKK (Supp. Figure 2).

Generation and functional characterization of HSulf-2 mutants

To investigate the functional relevance of the two putative HS binding sites identified using the cross-linking approach, we generated enzyme mutants, in which lysine residues of the VKEK and LKKK motifs were replaced by alanines. Alanine substitutions were introduced by site-directed mutagenesis to generate plasmids encoding two single motif mutants HSulf-2/VAEA, HSulf-2/LAAA and the double-mutant HSulf-2/VAEA/LAAA. As for HSulf-2 WT, vectors were used to stably transfect HEK293 cells. Enzymes were then recovered from the conditioned medium and purified as described above, with no changes in the expression yields and purification procedure.

We first sought to determine whether these mutations affected the enzyme arylsulfatase activity, using the 4MUS assay. Results (Fig. 4a and Supp. Figure 3B) showed equivalent fluorescence signal levels for WT and all mutant enzymes, indicating that neither VKEK nor LKKK epitopes are involved in HSulf arylsulfatase activity. We next compared the ability of WT and mutant HSulf-2 to bind to

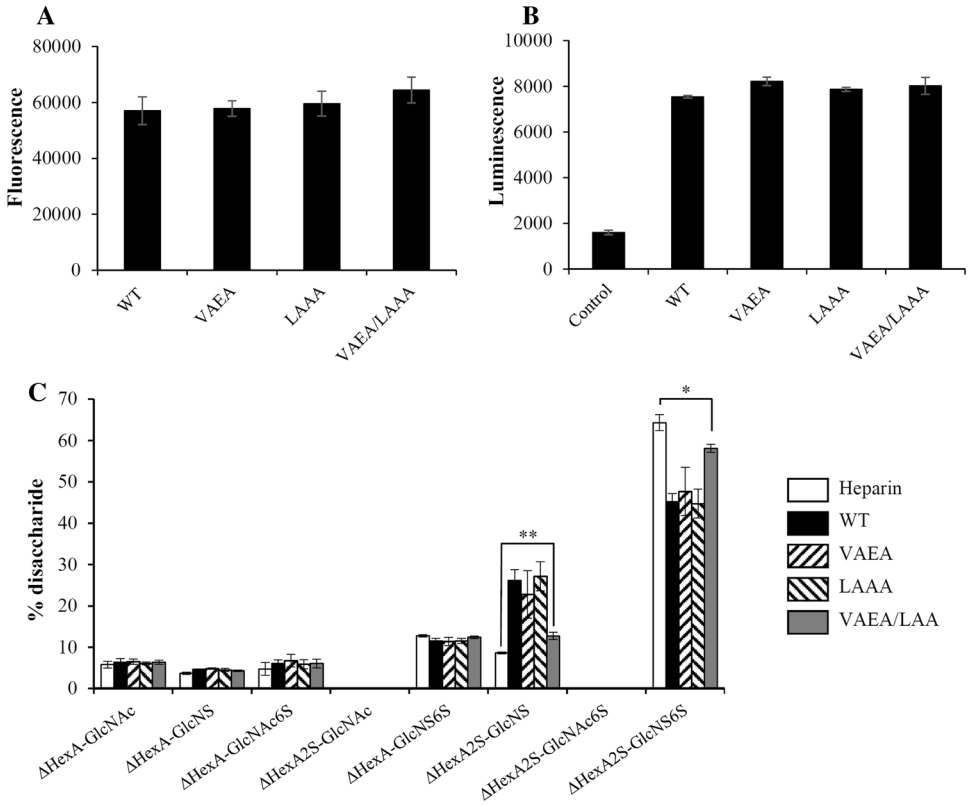

Fig. 4 Comparison of HSulf-2 and HSulf-2 mutants' biological activities. Analysis of the 4-MUS (**a**), heparin binding (**b**) and 6-*O*-endosulfatase (**c**) activities of WT HSulf-2 and mutants. Error bars represent SEM of triplicate analysis

heparin in our immunoassay. Results showed that all forms tested effectively bound to the polysaccharide (Fig. 4b). A K_D of 4.7 ± 3.6 nM was determined for the interaction of HSulf-2/VAEA/LAAA to heparin (Supp. Figure 4), an affinity very similar to that exhibited by HSulf-2 WT (Fig. 3c). Noteworthy, introduction of the VAEA/LAAA mutations in the HSulf-2ΔHD truncated form significantly reduced, but did not completely abolish binding (Supp. Figure 4). Altogether, these data suggest that HSulf-2 VKEK and LKKK epitopes are primarily responsible for the low-affinity HS binding property of the enzyme CAT domain (although other residues within this domain may also be involved), but contribution of these motifs to the interaction of the full-length enzyme with the polysaccharide is negligible compared to that of the HD domain.

HS 6-*O*-endosulfatase activity was finally assessed, as described above (Fig. 4c). When compared to HSulf-2 WT, treatment with HSulf-2/VAEA and HSulf-2/LAAA yielded very similar composition profile. In contrast, HSulf-2/VAEA/LAAA double mutant led to drastically reduced changes in heparin disaccharide composition, with attenuated but significant 6.2% reduction and 4.1% increase in [ΔHexA(2S)-GlcNS(6S)] and [ΔHexA(2S)-GlcNS] disaccharide content, respectively. Importantly, these results indicate that combined mutations of VKEK and LKKK epitopes significantly reduce, but do not abrogate the enzyme 6-*O*-endosulfatase activity. In agreement with this, we found that increased 6-*O*-desulfation of heparin by HSulf-2/VAEA/LAAA could be achieved using more extensive digestion conditions (data not shown).

Conservation of the CAT domain HS-binding sites within sulfatases

In light of these observations, we then studied the conservation of these newly identified functional epitopes amongst sulfatases (Fig. 5). Despite significant homology of Sulf CAT domain with other sulfatases, VKEK and LKKK like sequences were only found in Sulf isoforms and orthologs, thus supporting further a contribution to the specific HS 6-*O*-endosulfatase activity of these enzymes. Noteworthy, HSulf-2 K_{402} of the L_{401}KKK motif was only conserved in Sulf-2 orthologs and replaced by an asparagine in Sulf-1. This could either suggest that this residue could be involved in Sulf-2 isoform-specific processing of HS substrate, or may not play any relevant role. Similarly, residue at position 179 of the V_{179}KEK motif was consistently a non-polar amino acid in mammalian Sulfs (V for Sulf-2 or I for Sulf-1), but was substituted by an asparagine in Quail Sulf-1 (QSulf-1). Finally, it is worth noting that Glucosamine 6-sulfatase exhibits three basic residues aligning with HSulf-2 VKEK motif, which may suggest that this epitope could partly participate to the specific recognition of glucosamine 6-sulfate residues.

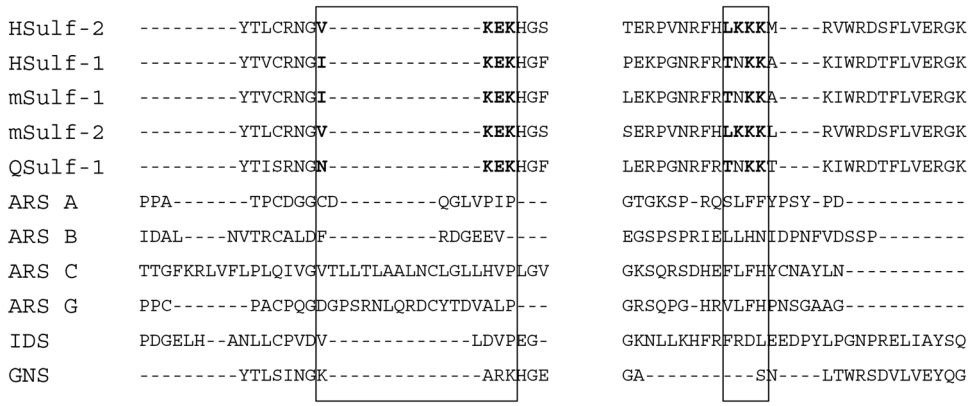

Fig. 5 Conservation of CAT HS binding epitopes within sulfatases. Clustal omega sequence alignment of HSulf-2 and HSulf-1; mouse Sulf-1 and -2 (mSulf-1 and mSulf-2, respectively); quail Sulf-1 (QSulf-1); human arylsulfatase (ARS) A, B, C and G; human iduronate 2-sulfatase (IDS) and human Glucosamine 6-sulfatase (GNS). Sequences aligned with HSulf-2 VKEK and LKKK epitopes are framed and conserved residues within these motifs are in bold

Molecular modelling of heparin–HSulf-2 Cat-domain interaction

To provide a structural basis for the underlying mechanism, we used HSulf-2 CAT domain homology with sulfatase of known structure to model the interaction of the VKEK and LKKK epitopes with a heparin oligosaccharide. The spatial structure of HSulf-2ΔHD was built on the base of three human arylsulfatases alignment. The sequences of three arylsulfatases share 29–36% of identity and demonstrate common folding. CAT-domain of Sulf2 reveals 26–28% of identity toward these arylsulfatases. Resulted model structure was quality controlled with following output (corresponding values for the template structure are given in parenthesis): G-factors overall −0.26 (−0.14), covalent −0.41 (−0.22), dihedrals −0.18 (−0.15), torsions in favorable regions were 82.6% (86.8), in allowed 14% (11.9), in generously allowed 2.6% (1.1) and in disallowed regions 0.9% (0.3). The model indicated the alignment of L_{401}KKK, FGly and V_{179}KEK within a groove of the protein surface, forming a binding site (Fig. 6a). The distance between the fragments L_{401}KKK and V_{179}KEK, calculated for Cα atoms belonging to K_{404} and K_{180}, amounts to 32 Å and could thus accommodate an octasaccharide (Fig. 6b). Given the 6-sulfate of the GlcNS(6S) in +1 position facing the catalytic FGly, the GlcNS(6S) in −4 position is in front of K_{404}, thereby establishing an electrostatic contact between the 6-sulfate and the lysine side chain amino group. Furthermore, the IdoA(2S) in +3 position occurs next to K_{180} forming a salt bridge between the 2-sulfate group and the amino group of lysine. A longer oligosaccharide, GlcNS(6S)-[IdoA(2S)-GlcNS(6S)]$_5$, is required to grasp both lysines in V_{179}KEK fragment of the binding site. Herein, an additional salt bridge is formed between the 2-sulfate of the GlcNS(6S) in +6 position and the amino group of the K_{182}.

Discussion

Whereas all other sulfatases take part in the cellular catabolism of sulfated compounds, enzymes of the Sulf sub-family have been associated with major regulatory processes. This

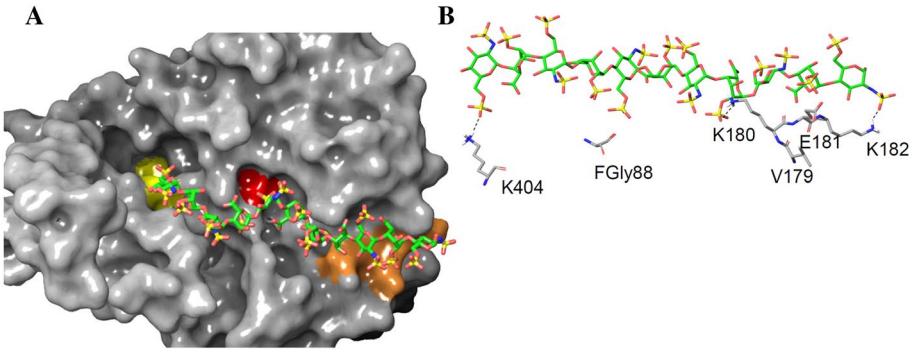

Fig. 6 Modeling of the HSulf-2ΔHD in complex with a heparin oligosaccharide. The surface representation of HSulf-2ΔHD model with the ligand GlcNS(6S)-[IdoA(2S)-GlcNS(6S)]$_5$ bound. Catalytic cysteine modified FGly (C88) is highlighted in red and the residues of V_{179}KEK and L_{401}KKK sequences identified using the cross-linking mapping approach are shown in orange and yellow, respectively (**a**). View of protein–HS ligand complex showing the minimal length unit required for efficient binding of two epitopes. Color coding is the following: C atoms—grey for the protein and green for the ligand; N atoms—blue, O atoms—red, S atoms—yellow, H atoms (given only for lysine amino groups)—white (**b**)

functional specificity is both due to the complex nature of their HS polysaccharide substrate, which binds and modulates a multitude of protein ligands, and to their endosulfatase nature (other sulfatases are exoenzymes) that confers them ability to target and edit 6-*O*-sulfation pattern of HS functional S-domains. In addition, we have recently shown that HSulfs catalyzed HS 6-*O*-desulfation, through an original, processive and orientated mechanism [13]. All these unique features clearly suggest a highly complex mode of enzyme–substrate recognition, which largely remains to be clarified. However, mechanistic and structural studies of Sulfs remain scarce and have been limited to the difficulty to achieve preparation of pure recombinant and functional enzymes. We report here for the first time the preparation of purified, recombinant HSulf-2, which was achieved by expressing the enzyme in mammalian HEK293F cells adapted to culture in suspension. Such system facilitated purification of HSulf-2 from a conditioned medium depleted in protein contaminants (HEK293F cells are grown in serum-free medium), and guaranteed the integrity of Hsulf post-translational modifications, as demonstrated by mass spectrometry proteomic analysis (Seffouh et al., submitted). Surprisingly, attempts to purify the protein through its 6xHis C-terminal tag were unsuccessful, suggesting that the C-Terminal end of the protein may not be available within the folded protein. Nevertheless, efficient purification could be achieved using standard ion-exchange and size exclusion chromatography procedures. Noteworthy, yields for the preparation of full-length purified (90–95% purity) HSulf-2 reached ~ 2 to 3 mg/L of culture medium, a figure that now opens new perspectives of studying HSulf-2 through material demanding biophysical and structural analysis techniques. Intriguingly, HSulf-2 full-length protein eluted with a high aMW, while the HSulf-2ΔHD mutant (i.e. HSulf-2 lacking its HD domain) showed size-exclusion elution time in accordance with predicted aMW (data not shown). In addition, the C-terminal chain of the enzyme including most of the HD domain could not be visualized by Coomassie blue-stained PAGE (Fig. 1c). These observations along with our proteomic analysis data (Seffouh et al., submitted) clearly suggest unusual structural properties within the HD domain. We speculate that this domain could feature an unusually extended conformation and/or multiple *N*-glycosylation/post-translational modifications, which would significantly increase the hydrodynamic radius of the whole protein. In addition, the detection of HSulf-2 degradation products, most likely within the HD domain, suggests propensity to proteolysis (contrary to the CAT domain), in line with secondary structure predictions based on amino-acid sequence, which indicated the presence of unstructured regions within the HD domain. Further investigations will be needed to clarify HD unexpected structural and functional behavior.

Consistently with previous studies performed on concentrated CM [10, 11, 13], the purified recombinant HSulf-2 showed all expected biological activities. We first demonstrated that the enzyme retained the ability to process the fluorogenic 4MUS pseudo-substrate, which is the hallmark of arylsulfatase activity (Fig. 2a). We also confirmed that HSulf-2 productively bound to heparin (Fig. 3). SPR analysis of HSulf-2 interaction with heparin (Fig. 3a, b) showed formation of very stable enzyme/polysaccharide complexes (limited loss of signal during the dissociation phase). Noteworthy, data could not be fitted to a Langmuir binding model. This evidenced a complex mode of interaction, in agreement with previous data suggesting the contribution of multiple and dynamic binding events within Sulf HD/heparin interaction [19]. As dynamic binding measurements failed to provide reliable kinetic parameters, binding K_D was determined by ELISA, which confirmed the expected high affinity (~ 4 nM) of HSulf-2 for heparin (Fig. 3c). Finally, we demonstrated the ability of recombinant, purified HSulf-2 to 6-*O*-desulfate heparin (Fig. 2b). In agreement with published data obtained with concentrated CM, the purified full-length enzyme essentially targeted the heparin [ΔHexA(2S)-GlcNS(6S)] trisulfated disaccharide, although residual activity could also be observed on [ΔHexA-GlcNS(6S)] disaccharides. Noteworthy, removal of tags upon TEV treatment had no effect on HSulf-2 activity (data not shown).

In contrast with full-length HSulf-2, the HSulf-2ΔHD form was efficiently retained by nickel column chromatography (Supp. Figure 1B), thus suggesting a contribution of the HD domain in burying the C-terminal domain within the native structure. Yields obtained were also significantly higher. We assume that this could be due to a reduced retention of the enzyme by cell-surface HS, in agreement with studies highlighting the HD domain as the major cell-surface binding component [11]. HSulf-2ΔHD exhibited similar 4MUS activity (Fig. 2a), but with a shorter initial velocity period (Supp. Figure 3A). This discrepancy should be investigated further and may indicate a role of the HD domain in the stability of the enzyme. In contrast, HSulf-2ΔHD exhibited strongly reduced heparin binding (Fig. 3) and 6-*O*-endosulfatase activity (Fig. 2b). This is consistent with the critical role played by the HD domain in the interaction with HS substrate. However, it is worth noting that residual binding and activity could still be noted, thus suggesting that the HD domain significantly contributes but may not be strictly required for the enzyme 6-*O*-endosulfatase activity and that additional HS binding sites may be found within the enzyme CAT domain.

Altogether, these data validated the functional integrity of recombinant purified HSulf-2 and ruled out the possibility of additional partners possibly present in concentrated medium preparations, which could play a role in the binding and/or processing of HS. We also further confirmed

previous indications that HSulf-2 CAT and C-ter domains (i.e. HSulf-2ΔHD) comprised all necessary features required for a functional arylsulfatase active site [12], and that Sulf HD domain plays a major role in high-affinity binding to HS heparin [11, 12, 27].

We next took advantage of this newly available source of purified HSulf-2 to clarify the molecular determinants involved in the enzyme–substrate recognition process. Because of the abundance of basic residues within Sulf amino acid sequence (127 K and R residues for HSulf-2), identification of HS binding domains could not readily be investigated through conventional alanine scanning site directed mutagenesis approaches. We thus addressed this issue, using a previously developed cross-linking technique to map HS binding sites [20]. Briefly, this technique is based on the generation of protein/heparin bead covalent complexes, the proteolytic digestion of these complexes and the identification of peptides remaining bound to the heparin (i.e. comprising the heparin binding site) by N-terminal sequencing. A first examination of HD highly basic 299 amino acid sequence revealed the presence of 2 putative Cardin-Weintraub HS binding motifs [28]: R_{518}RKKLFKKKYK and K_{703}RKKKLRKLLKR. However and although this technique has been successfully applied to the study of many different heparin binding proteins over the years, analysis of HSulf-2 yielded unexpected results. The first cycles of sequencing showed high background level and recovery yields dropped very rapidly. Consequently, no HS binding sequence could be clearly identified within the HD domain. A likely explanation of this is the presence of too many different peptides cross-linked to the heparin to allow unambiguous amino acid attribution. We thus speculate that heparin covalently bound to many amongst the HD 41 NHS-activable lysine residues and that this interaction may not simply involve the two putative Cardin–Weintraub HS binding motifs. This again is in agreement with studies, showing that interaction of HS with HSulf HD domain was highly dynamic and involved multiple binding sites [19, 29]. Furthermore, generation of very short peptides also supports further a high susceptibility of this domain to enzyme proteolysis and the presence of large poorly structured regions within the HD domain. Nevertheless, our cross-linking strategy enabled identification of 2 epitopes present within the enzyme CAT domain: V_{179}KEK and L_{401}KKK. We thus generated mutants lacking each (or both) of these domains and analyzed their enzymatic activity. Data obtained showed no difference between HSulf-2 wild-type and mutant forms in the 4MUS assay (Fig. 4a and Supp. Figure 3B), suggesting that VKEK and LKKK epitopes were not part of the enzyme active site per se. Binding to heparin was not compromised either, which was expected as the HD domain is the major contributor to this interaction (Fig. 4b). Finally, we found very similar 6-*O*-endosulfatase activities for wild-type and single mutants, whereas HSulf-2 VAEA/LAAA double mutant exhibited dramatically reduced ability to 6-*O*-desulfate heparin (Fig. 4c). These results thus suggest that VKEK/LKKK epitopes are not required for the endosulfatase activity, but cooperatively contribute to its efficiency. These experimental data were reinforced by analysis of sulfatase sequences, which showed that these motifs were only conserved in Sulf orthologs (Fig. 5).

We next modelled HSulf-2ΔHD in complex with a GlcNS(6S)-[IdoA(2S)-GlcNS(6S)]$_5$ heparin oligosaccharide. The validity of such model is strongly supported by the sequence homology between HSulf-2 CAT domain and structure-solved arylsulfatases (A, B and C), which all share a conserved protein core folding. In absence of structural data, it should nevertheless be pointed out that the presence of the HD domain could impact the CAT domain structure in the context of the whole protein. However, we can speculate that a partially unstructured HD would have minor effects over the structure of the well-folded CAT domain. Our model showed alignment of the VKEK and LKKK epitopes with active site FGly residue, and that an octasaccharide could span over all three motifs. As model calculations were made on the basis of rigid proteins, we anticipate that potential local flexibility could slightly affect the distance between the VKEK and LKKK motifs. Precise determination of the oligosaccharide size will thus require further experimental evidence. However, this suggests that VKEK and LKKK binding sites participate to the endosulfatase activity by enabling recognition and binding of larger HS motifs than the [IdoA(2S)-GlcNS(6S)] disaccharide substrate (Fig. 6). Noteworthy, non-conserved K_{402} of the L_{401}KKK motif did not establish contact with the oligosaccharide, which supports the hypothesis that this residue is not involved in the binding.

On the basis of these data, we refined our previously published model [13] to explicit HSulf desulfation mechanism (Fig. 7). In this model, HSulf primary high-affinity interaction occurs through the enzyme HD domain. However, VKEK and LKKK epitopes contribute further to this interaction by guiding and properly aligning the polysaccharide towards the enzyme active site (Fig. 7a). In the absence of these motifs, productive interaction still occurs, but desulfation is inefficient due to improper presentation of the polysaccharide to the active site (Fig. 7b). Processing of small pseudo-substrates such as 4-MUS are unaffected by the removal of VKEK/LKKK motifs, as these access directly to the active site. In absence of the HD, affinity of the enzyme for HS is significantly reduced and impairs subsequent 6-*O*-desulfation (Fig. 7c).

In conclusion, we describe here a novel, robust and efficient system to produce functional, purified recombinant Sulfs. This new source of enzyme enabled us to investigate and provide further insights into the structural basis

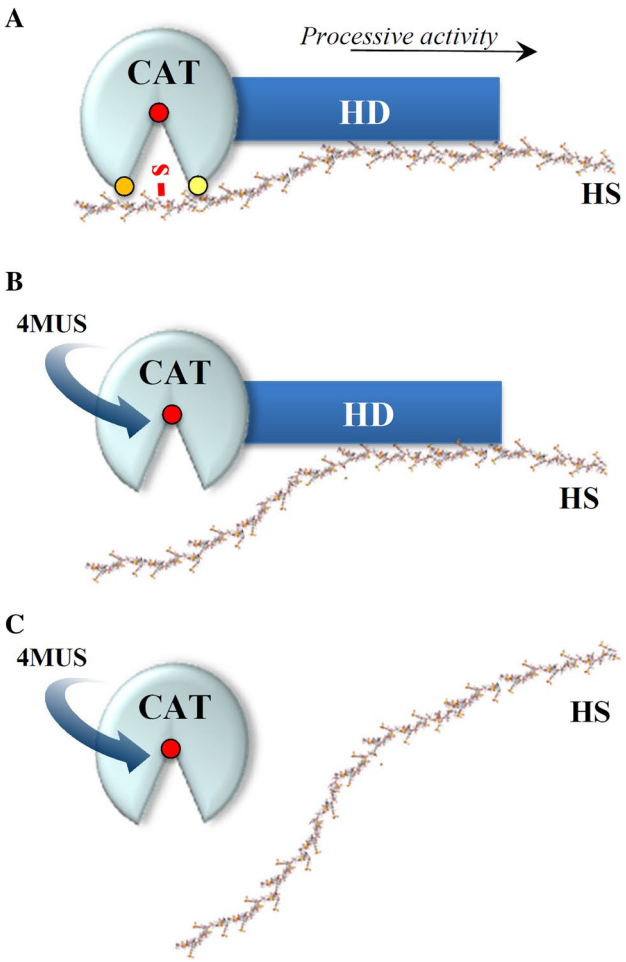

Fig. 7 Coordinated activity of CAT and HD domains for the binding and 6-*O*-desulfation of HS. For WT HSulf-2 (**a**), high-affinity binding to HS is mediated by the HD domain, while CAT domain VKEK (orange dot)/LKKK (yellow dot) HS binding sites contribute to efficient 6-*O*-desulfation by enabling presentation of the polysaccharide chain to the active site (FGly residue shown as a red dot). For HSulf-2/VAEA/LAAA mutant (**b**), high-affinity binding to HS still takes place, but the polysaccharide chain is not properly guided towards the active site, leading to impaired 6-*O*-endosulfatase activity. Processing of small 4-MUS pseudo-substrate remains unaffected. Further removal of the HD domain (**c**) leads to a HSulf-2ΔHD/VAEA/LAAA mutant unable to bind or process HS substrates

of HSulf-2 enzyme/substrate recognition. Based on our data, we propose here a refined model of the underlying mechanism that highlights the coordinated functions of Sulf CAT and HD domains, which constitutes a significant step forward towards the understanding of the highly complex and elusive enzymes. Finally, we foresee that access to purified recombinant Sulf with expression yield in the mg/L range should pave the way to new developments and major progress in the characterization of Sulf structure and molecular features, as well as for the screening and design of Sulf-specific inhibitors for potential application in cancer therapy.

Acknowledgements The authors would like to thank Elisa Tournebize for technical assistance, Marjolaine Noirclerc-Savoye for her precious advice on molecular biology, Philippe Desprès for providing the SNAP-containing shuttle vector and Kenji Uchimura for the Anti-HSulf-2 antibody. This work used the SPR, Robiomol and amino-acid sequencing platforms of the Grenoble Instruct centre (ISBG; UMS 3518 CNRS-CEA-UJF-EMBL) with support from FRISBI (ANR-10-INSB-05-02) and GRAL (ANR-10-LABX-49-01) within the Grenoble Partnership for Structural Biology (PSB). This work was also supported by the CNRS and the GDR GAG (GDR 3739), the "Investissements d'avenir" program Glyco@Alps (ANR-15-IDEX-02), and by grants from the Agence Nationale de la Recherche (ANR-12-BSV8-0023 and ANR-17-CE11-0040) and Université Grenoble-Alpes (UGA AGIR program).

References

1. Dhoot GK, Gustafsson MK, Ai X, Sun W, Standiford DM, Emerson CP Jr (2001) Regulation of Wnt signaling and embryo patterning by an extracellular sulfatase. Science 293:1663–1666
2. Sarrazin S, Lamanna WC, Esko JD (2011) Heparan sulfate proteoglycans. Cold Spring Harb Perspect Biol. https://doi.org/10.1101/cshperspect.a004952
3. Kjellén L, Lindahl U (2018) Specificity of glycosaminoglycan-protein interactions. Curr Opin Struct Biol 50:101–108. https://doi.org/10.1016/j.sbi.2017.12.011
4. Monneau Y, Arenzana-Seisdedos F, Lortat-Jacob H (2016) The sweet spot: how GAGs help chemokines guide migrating cells. J Leukoc Biol 99:935–953. https://doi.org/10.1189/jlb.3MR0915-440R
5. Li J-P, Kusche-Gullberg M (2016) Heparan sulfate: biosynthesis, structure, and function. Int Rev Cell Mol Biol 325:215–273. https://doi.org/10.1016/bs.ircmb.2016.02.009
6. Kreuger J, Kjellen L (2012) Heparan sulfate biosynthesis: regulation and variability. J Histochem Cytochem 60:898–907. https://doi.org/10.1369/0022155412464972
7. Vives RR, Seffouh A, Lortat-Jacob H (2014) Post-synthetic regulation of HS structure: the Yin and Yang of the sulfs in cancer. Front Oncol 3:331. https://doi.org/10.3389/fonc.2013.00331
8. Rosen SD, Lemjabbar-Alaoui H (2010) Sulf-2: an extracellular modulator of cell signaling and a cancer target candidate. Expert Opin Ther Targets 14:935–949. https://doi.org/10.1517/14728222.2010.504718
9. Nishitsuji K (2018) Heparan sulfate S-domains and extracellular sulfatases (Sulfs): their possible roles in protein aggregation diseases. Glycoconj J. https://doi.org/10.1007/s10719-018-9833-8
10. Morimoto-Tomita M, Uchimura K, Werb Z, Hemmerich S, Rosen SD (2002) Cloning and characterization of two extracellular heparin-degrading endosulfatases in mice and humans. J Biol Chem 277:49175–49185
11. Frese MA, Milz F, Dick M, Lamanna WC, Dierks T (2009) Characterization of the human sulfatase Sulf1 and its high affinity heparin/heparan sulfate interaction domain. J Biol Chem 284:28033–28044
12. Tang R, Rosen SD (2009) Functional consequences of the subdomain organization of the sulfs. J Biol Chem 284:21505–21514
13. Seffouh A, Milz F, Przybylski C, Laguri C, Oosterhof A, Bourcier S, Sadir R, Dutkowski E, Daniel R, van Kuppevelt TH, Dierks T, Lortat-Jacob H, Vives RR (2013) HSulf sulfatases catalyze processive and oriented 6-*O*-desulfation of heparan sulfate that differentially regulates fibroblast growth factor activity. Faseb J 27:2431–2439. https://doi.org/10.1096/fj.12-226373
14. Pempe EH, Burch TC, Law CJ, Liu J (2012) Substrate specificity of 6-*O*-endosulfatase (Sulf-2) and its implications in synthesizing

anticoagulant heparan sulfate. Glycobiology 22:1353–1362. https://doi.org/10.1093/glycob/cws092
15. Nagamine S, Tamba M, Ishimine H, Araki K, Shiomi K, Okada T, Ohto T, Kunita S, Takahashi S, Wismans RG, van Kuppevelt TH, Masu M, Keino-Masu K (2012) Organ-specific sulfation patterns of heparan sulfate generated by extracellular sulfatases Sulf1 and Sulf2 in mice. J Biol Chem 287:9579–9590. https://doi.org/10.1074/jbc.M111.290262
16. Lamanna WC, Baldwin RJ, Padva M, Kalus I, Ten Dam G, van Kuppevelt TH, Gallagher JT, von Figura K, Dierks T, Merry CL (2006) Heparan sulfate 6-*O*-endosulfatases: discrete in vivo activities and functional co-operativity. Biochem J. 400:63–73
17. Lamanna WC, Frese MA, Balleininger M, Dierks T (2008) Sulf loss influences *N*-, 2-*O*-, and 6-*O*-sulfation of multiple heparan sulfate proteoglycans and modulates fibroblast growth factor signaling. J Biol Chem 283:27724–27735
18. Milz F, Harder A, Neuhaus P, Breitkreuz-Korff O, Walhorn V, Lubke T, Anselmetti D, Dierks T (2013) Cooperation of binding sites at the hydrophilic domain of cell-surface sulfatase Sulf1 allows for dynamic interaction of the enzyme with its substrate heparan sulfate. Biochim Biophys Acta. https://doi.org/10.1016/j.bbagen.2013.07.014
19. Harder A, Möller A-K, Milz F, Neuhaus P, Walhorn V, Dierks T, Anselmetti D (2015) Catch bond interaction between cell-surface sulfatase Sulf1 and glycosaminoglycans. Biophys J 108:1709–1717. https://doi.org/10.1016/j.bpj.2015.02.028
20. Vives RR, Crublet E, Andrieu JP, Gagnon J, Rousselle P, Lortat-Jacob H (2004) A novel strategy for defining critical amino acid residues involved in protein/glycosaminoglycan interactions. J Biol Chem 279:54327–54333
21. Henriet E, Jäger S, Tran C, Bastien P, Michelet J-F, Minondo A-M, Formanek F, Dalko-Csiba M, Lortat-Jacob H, Breton L, Vivès RR (1861) A jasmonic acid derivative improves skin healing and induces changes in proteoglycan expression and glycosaminoglycan structure. Biochim Biophys Acta Gen Subj 2017:2250–2260. https://doi.org/10.1016/j.bbagen.2017.06.006
22. Vives RR, Sadir R, Imberty A, Rencurosi A, Lortat-Jacob H (2002) A kinetics and modeling study of RANTES(9-68) binding to heparin reveals a mechanism of cooperative oligomerization. Biochemistry (Mosc.) 41:14779–14789
23. Sali A, Blundell TL (1993) Comparative protein modelling by satisfaction of spatial restraints. J Mol Biol 234:779–815. https://doi.org/10.1006/jmbi.1993.1626
24. Laskowski RA, Rullmannn JA, MacArthur MW, Kaptein R, Thornton JM (1996) AQUA and PROCHECK-NMR: programs for checking the quality of protein structures solved by NMR. J Biomol NMR 8:477–486
25. Dominguez C, Boelens R, Bonvin AMJJ (2003) HADDOCK: a protein-protein docking approach based on biochemical or biophysical information. J Am Chem Soc 125:1731–1737. https://doi.org/10.1021/ja026939x
26. van Zundert GCP, Rodrigues JPGLM, Trellet M, Schmitz C, Kastritis PL, Karaca E, Melquiond ASJ, van Dijk M, de Vries SJ, Bonvin AMJJ (2016) The HADDOCK2.2 Web server: user-friendly integrative modeling of biomolecular complexes. J Mol Biol 428:720–725. https://doi.org/10.1016/j.jmb.2015.09.014
27. Ai X, Do AT, Kusche-Gullberg M, Lindahl U, Lu K, Emerson CP Jr (2006) Substrate specificity and domain functions of extracellular heparan sulfate 6-*O*-endosulfatases, QSulf1 and QSulf2. J Biol Chem 281:4969–4976
28. Cardin AD, Weintraub HJ (1989) Molecular modeling of protein-glycosaminoglycan interactions. Arteriosclerosis 9:21–32
29. Walhorn V, Möller A-K, Bartz C, Dierks T, Anselmetti D (2018) Exploring the sulfatase 1 catch bond free energy landscape using Jarzynski's equality. Sci Rep 8:16849. https://doi.org/10.1038/s41598-018-35120-0

Publisher's Note Springer Nature remains neutral with regard to jurisdictional claims in published maps and institutional affiliations.